

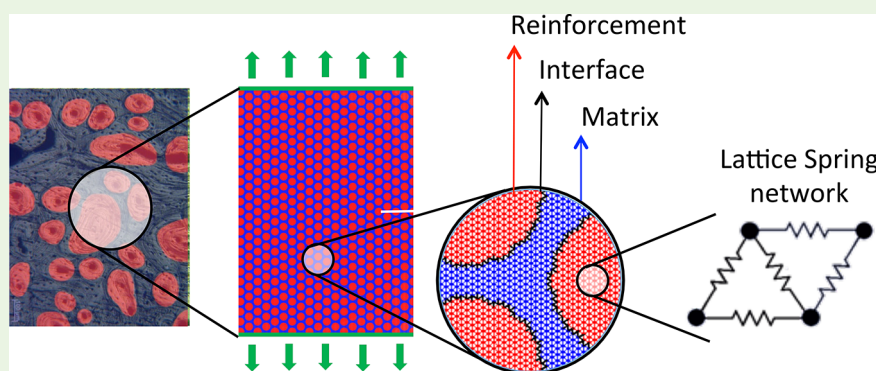
Computational Framework to Predict Failure and Performance of Bone-Inspired Materials

Flavia Libonati,^{†,‡} Vito Cipriano,[†] Laura Vergani,[†] and Markus J. Buehler^{*,‡,§}

[†]Department of Mechanical Engineering, Politecnico di Milano, via La Masa 1, 20156 Milano, Italy

[‡]Laboratory for Atomistic and Molecular Mechanics (LAMM), Department of Civil and Environmental Engineering, Massachusetts Institute of Technology, 77 Massachusetts Avenue, Cambridge, Massachusetts 02139, United States

 Supporting Information



ABSTRACT: Bone and its substructures have recently been a source of inspiration for the design of novel composites, offering optimal strength-toughness and stiffness-density combinations, traits endowed by the abundance of complex biointerfaces. Bone-inspired design combined with engineering principles may offer a path toward reaching an optimal strength-toughness balance in new materials. On the one hand, with the advent of micro- and nanoreinforcements and novel manufacturing techniques, new possibilities for advanced materials have opened. On the other hand, the endeavor for novel materials with radically improved properties is spurring the research toward accurate and versatile numerical models to be used in the design phase. In this work, we present a 2D lattice spring model to predict the performance of previously tested 3D-printed bone-inspired composites, and their failure modes. The model has the capacity to correctly estimate the material performance and to reproduce the bonelike toughening mechanisms, occurring at different length scales in our composites. The numerical results show how the material properties, the interfaces, the reinforcement geometry, and the topological pattern affect the stress distribution and the propagation of defects, significantly decreasing the flaw sensitivity of the material. Our framework could be used for the design of new materials with improved fracture resistance and balance with stiffness and strength.

KEYWORDS: *bioinspired, 3D printing, modeling, toughening mechanisms, fracture, interfaces*

1. INTRODUCTION

Nature offers several examples of effective design for structural materials, with a palette of lightweight structural biological composites that often show a combination of properties, unmatched in engineering materials.^{1–4} The idea of composites—a framework by which internal interfaces are created to separate multiple material phases—comes from nature, where few universal building blocks (i.e., proteins and minerals) with meager base properties combine, through interfaces, to create several hierarchical substructures. The latter generate multiscale complex structures that yield outstanding mechanical properties, e.g., toughness and strength, which are several orders of magnitude larger than those of the base constituents.^{5–13}

The ever-increasing need for high performance (i.e., optimal combination of properties in terms of strength-toughness and stiffness-toughness) and low weight spurs the researchers to look at Nature and its optimized structures to find inspiring

models for new materials.¹⁴ In particular, bone and its substructures (e.g., brick-and-mortar structure at mesoscale, Haversian or osteon-like microstructure, foamlike trabecular structure) have recently been a source of inspiration for the design of novel composites, offering optimal strength-toughness and stiffness-density trade-offs.^{11,15–21} Bone-inspired design combined with engineering principles may offer a path toward reaching an ideal strength-toughness balance in new composite materials.

Recent advances in computer-assisted design (CAD) and additive manufacturing, together with novel numerical approaches, provide the possibility of designing ad hoc tunable and multifunctional composite materials for various applica-

Received: August 22, 2017

Accepted: October 26, 2017

Published: October 26, 2017

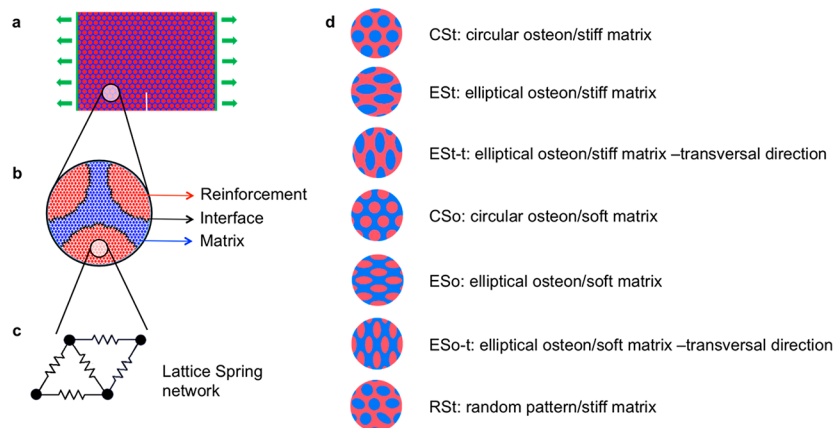


Figure 1. Schematic of the model: (a) schematic of the sample for in silico testing; (b) schematic of the composite pattern and the different materials (each color corresponds to a spring type, with its characteristic stiffness and elongation at breakage); (c) lattice spring network adopted to discretize the material; (d) topologies studied and corresponding nomenclatures.

tions that range from structural to optical and electrical, which is an exciting opportunity either for research or industry.^{3,15,18,22–25}

With the advent of pioneering manufacturing techniques, new possibilities for advanced materials have opened. However, the endeavor to discover novel materials with fundamentally improved properties puts the needs for versatile numerical models to be used in the design phase. Reliable numerical approaches are crucial to guide the design phase, whereas additive manufacturing can be used as proof-of-concept, to prove the validity of proposed composite materials and topologies.

In the literature,^{26–32} finite element models (FEMs) and lattice spring models (LSMs) are considered the principal numerical approaches to analyze the continuum mechanics of materials microstructures.

FEMs generally require preprocessed mesh generation, including mesh refinement in the area of particular interest, such as interfaces or crack tip. Some authors have used FEMs to elucidate the effect of topological features of biological and bioinspired materials.^{23,27,33} Besides FEMs, XFEMs (extended FEMs) have been recently adopted for the study of crack initiation and propagation phenomena in biological and composite materials.^{11,26,31,34,35} XFEM is a mesh independent method, which lets one model a propagating crack without using a focused mesh and without any previous information on crack location, solving the issue of time-consuming remeshing procedures. FE-based methods are generally reliable and cost-effective, and can also include nonlinearities due to the materials. However, they cannot provide information on the toughening mechanisms, occurring at different length scales.

LSMs have been widely used to simulate deformation and fracture problems, especially in heterogeneous materials, avoiding the demanding phase of mesh generation. Simulations, based on a coarse-grain description of the matter through a lattice spring design, are also very powerful as they can provide an insight into the material behavior, offering information on the deformation and fracture mechanisms and on the overall performance. In silico tests, representing a virtual reproduction of the experimental counterparts, allow one to follow the deformation and fracture process, along with toughening mechanisms occurring at different length scales. These discrete models, known in the literature with different names, e.g., coarse-grain m., spring network m., lattice spring m., are

versatile and could be applied to a wide series of materials and systems.^{28–30,36–39} These models have proven to be suitable to describe the fracture behavior of heterogeneous materials. In particular, a spring-network model has been developed by Curtin and Scher²⁸ to describe the effect of a distributed disorder on brittle fracture, finding an interesting brittle-to-ductile transition in the macroscopic stress-strain behavior with growing disorder. A simplified scalar lattice model, based on a 2D square lattice structure, has also been used to investigate the effect of mutual yielding-rehardening on reducing the stress concentration and enhancing the fracture toughness, providing generic insights into a range of natural and synthetic tough materials.³⁶ Plasticity effects have been introduced into these models, by locally decreasing the stiffness while maintaining stress continuity.²⁹ Mesoscale simulations have also been used to investigate the effect of structural hierarchies on the toughness and flaw sensitivity of biomineralized materials,³⁰ and multiscale 2D-composites,³⁷ then to elucidate the key design mechanisms of various bioinspired composite topologies and the role of the stiffness ratio of their constituents, to guide the manufacturing phase.³⁸

Here, we present a numerical framework based on a 2D lattice spring model (Figure 1a–c) able to predict the performance of various 3D-printed bone-inspired composites (Figure 1d), and their failure modes. The composite topologies are inspired by the Haversian structure of cortical bone and consist of a pattern of circular and elliptical cylinders, aimed at mimicking the osteon, a characteristic feature of bone, interspersed into a matrix. The model, validated on previous experimental results,¹⁵ is able to correctly estimate the material performance and the toughening and failure mechanisms, and it could be used for the design of new tunable materials with improved fracture resistance and balance with stiffness and strength. Moreover, the 2D model would also be suitable for the simulation of emergent 2D materials systems, e.g., graphene, MoS₂ (molybdenum disulfide).

2. MATERIALS AND METHODS

2.1. Model. To predict the behavior of heterogeneous complex materials, we adopted a spring-bead model based on a 2D triangular lattice. Each bead in the lattice, representing a portion of the real sample, interacts with the nearest neighbors via harmonic springs. The model, whose framework is schematically represented in Figure S1, is calibrated on the basis of the outcome of a previous experimental

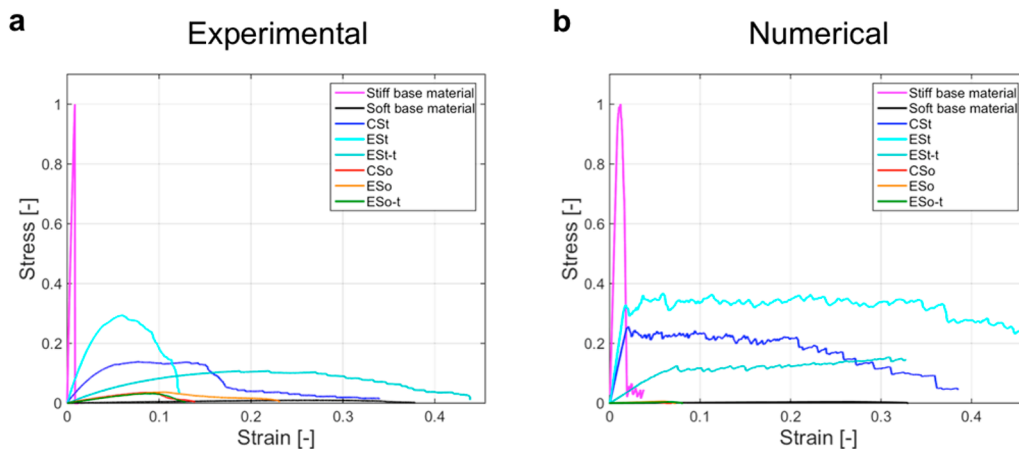


Figure 2. Stress–strain curves for the homogeneous base materials and the various composite topologies: a similar trend for experimental and numerical results can be observed. (a) Experimental curves: the stresses are normalized by the experimental strength of the Stiff base material. (b) Numerical curves: the stresses are normalized by the numerical strength of the stiff base material.

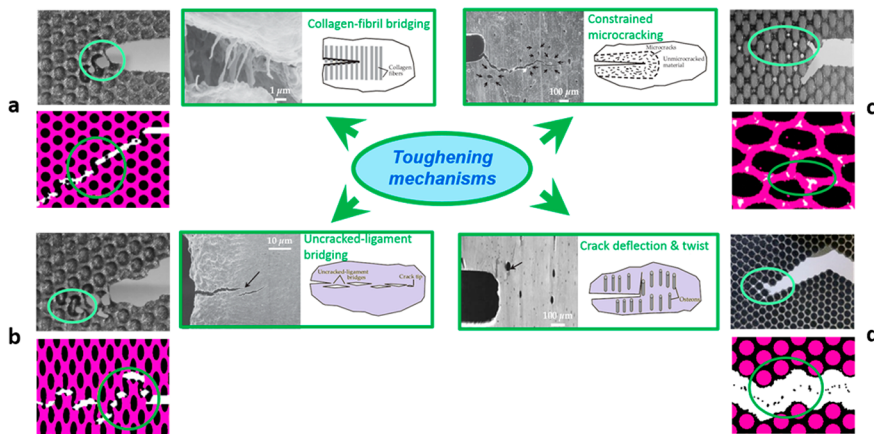


Figure 3. Prediction of the toughening mechanisms observed in the microstructure of cortical bone and mimicked in the 3D-printed materials. The characteristic toughening mechanisms occurring in bone microstructure, such as (a) fibril bridging behind the crack, (b) constrained microcracking ahead the crack tip region, (c) uncracked-ligament bridging, and (d) crack deflection and twist, have been correctly implemented into the 3D-printed bonelike composites, leading to an improvement in the overall toughness and strength of the materials. The numerical models are able to reproduce such mechanisms and accurately predict the failure modes experimentally observed. Black and white pictures showing the failure modes of 3D-printed bioinspired composite during testing are adapted with permission from ref 15. Copyright 2016 Wiley. Black and white figures showing microscopic images of bone failure mechanisms together with the corresponding schematic representation are adapted with permission from ref 40. Copyright 2009 American Institute of Physics.

campaign.¹⁵ First, we calibrated the material properties by performing *in silico* tests on homogeneous base materials (Figure S2). By adopting the same numerical framework, we simulated the behavior of a strip crack problem, implementing different patterns, aimed at reproducing various bone-inspired composite topologies.

2.2. Material Properties and Energy Landscape. We used the LAMMPS code to perform simulations of the strip crack problem aimed at reproducing the experimental setup described in ref 15. To describe the interactions between the beads, we adopted a harmonic potential, assigning a specific stiffness and elongation at breakage to each spring (the properties are provided as Supporting Information). To describe the composite nature of the samples, we assigned three different values of stiffness: (i) for the stiff phase, (ii) for the soft phase, and (iii) for the interphase. Although we are dealing with bimaterial composites, we assumed that during the additive manufacturing, the two materials at the interphase mixed before the UV-curing, hence creating a small interface layer with intermediate properties. This hypothesis is supported by evidence, as no interface failure has occurred during testing of composites. We defined the material properties (i.e., stiffness and elongation at breakage), based on the experimental outcome. We modeled the crack by means of zero-

stiffness springs. Each sample is included in a large simulation box with nonperiodic boundary conditions.

2.3. MD Simulations. The model was geometrically optimized through energy minimization, according to the conjugate gradient algorithm. Then the two edges were clamped and the sample relaxed under an NVE (microcanonical) ensemble. After equilibration of the system, the tests were performed in displacement-control mode, by using a quasi-static loading mode consisting of several increments, each one followed by long energy minimization steps (conjugate gradient algorithm). The loading–minimization cycles were run until failure occurred. A schematic of the sample with the applied loading conditions is provided in Figure S1, along with the simulation framework. As criterion for crack propagation, we used fix bond break command, allowing for bond breakage when surpassing the maximum displacement of the spring. Breaking a bond generally alters the energy of a system. A long minimization step allowed us to avoid a dramatic change in the energy of the system and a correct load transfer from the edges to the middle of the sample (see Figure S1), reducing the time gap between experimental and numerical testing.

2.4. Data Postprocessing. Data analysis was performed by means of visual molecular dynamics (VMD),⁴² allowing one to monitor the simulation while running, to observe the deformation and toughening

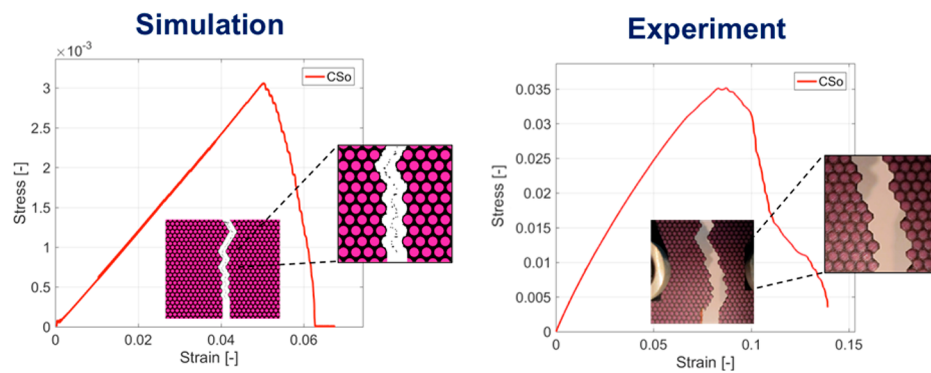


Figure 4. Comparison between numerical and experimental results in terms of stress–strain behavior and failure mode. The experimentally observed failure mode, here referred to the CS₀ composite topology (circular reinforcement and soft matrix), is accurately predicted by the simulations. The stress–strain trend is also replicated, but showing a one order of magnitude difference in stress due to the higher numerical stiffness assigned to the base materials. In both plots, the stress is normalized with respect to the numerical (left) and experimental (right) strength of the stiff base material.

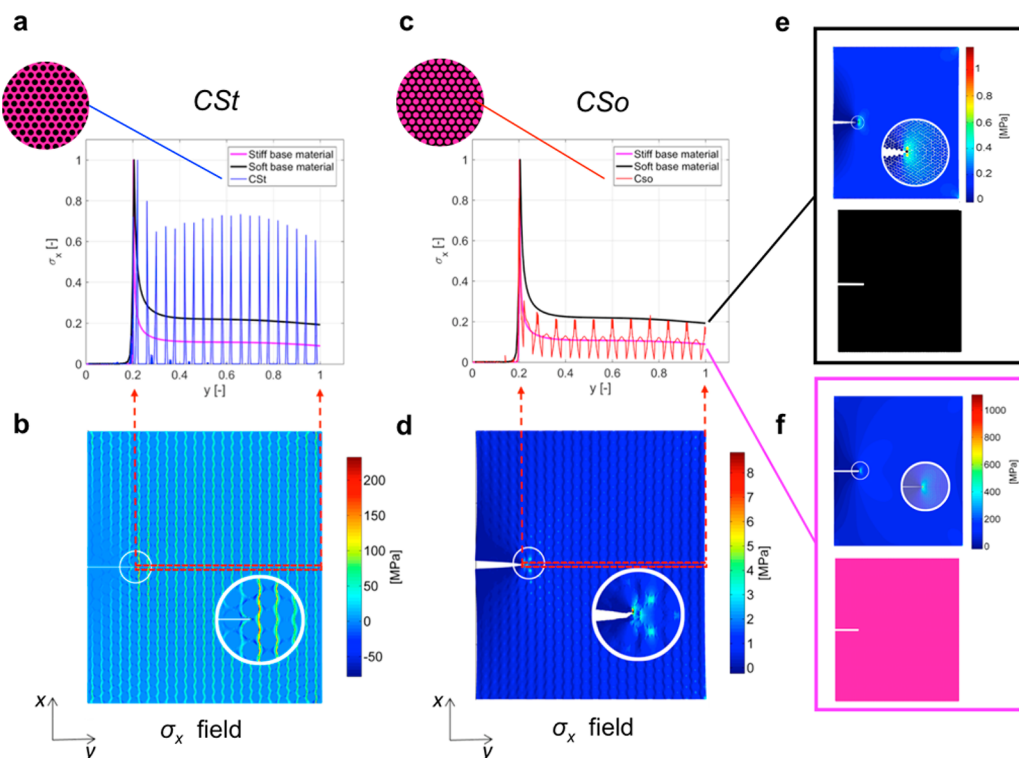


Figure 5. Matrix effect. The combination of circular topology and stiff matrix (CSt) shows to be beneficial for reducing the stress concentration at crack tip, especially if compared with the CS₀ topology (circular osteon/soft matrix) and with the stiff and soft base materials. Stress (σ_x) trend from the crack tip to the far field in (a) CSt and in (c) CS₀, showing stress delocalization due to the geometric pattern in both cases. The case of CSt also shows a reduced stress concentration at the crack tip with respect to the far field, if compared to CS₀ and to the homogeneous soft and stiff materials, making it more damage tolerant. (b, d) Map of the stress (σ_x) field and zoom-in around the crack tip in (b) CSt and in (d) CS₀. Highlighted with red dashed lines the area where the stresses, plotted in a and c, are calculated. The color-bar indicates the magnitude of the stress in MPa. (e, f) Maps of the stress field in the (e) soft and (f) stiff base materials and schematics of the single-edge cracked homogeneous samples.

mechanisms and the failure modes. The postprocessing of numerical data (e.g., stress and strains) was performed using MATLAB (Mathworks, Inc.). In the postprocessing we used the virial stress output from the simulations, and the engineering strain to get the stress–strain response. The mechanical properties (i.e., stiffness, strength, strain at failure, and toughness modulus etc.) are calculated from the stress–strain data. The toughness modulus is calculated as the area underneath the stress–strain curve. Stress maps are created by plotting the virial stresses^{45,46} on each bead, by means of MATLAB (Mathworks, Inc.).

3. RESULTS

3.1. Mechanical Properties. Figure 2 shows the experimental and numerical stress–strain trends for all the case studies. To name the various topologies we adopted the same nomenclature as in ref 15 to be thorough, the acronyms are also explained in Figure 1d. The numerical models reproduce the mechanical behavior of the various composite topologies. The predictions of the strains are accurate, whereas the numerical stresses are about one order of magnitude higher than the experimental ones, as expected. By normalizing the experimental and numerical stress results with respect to the

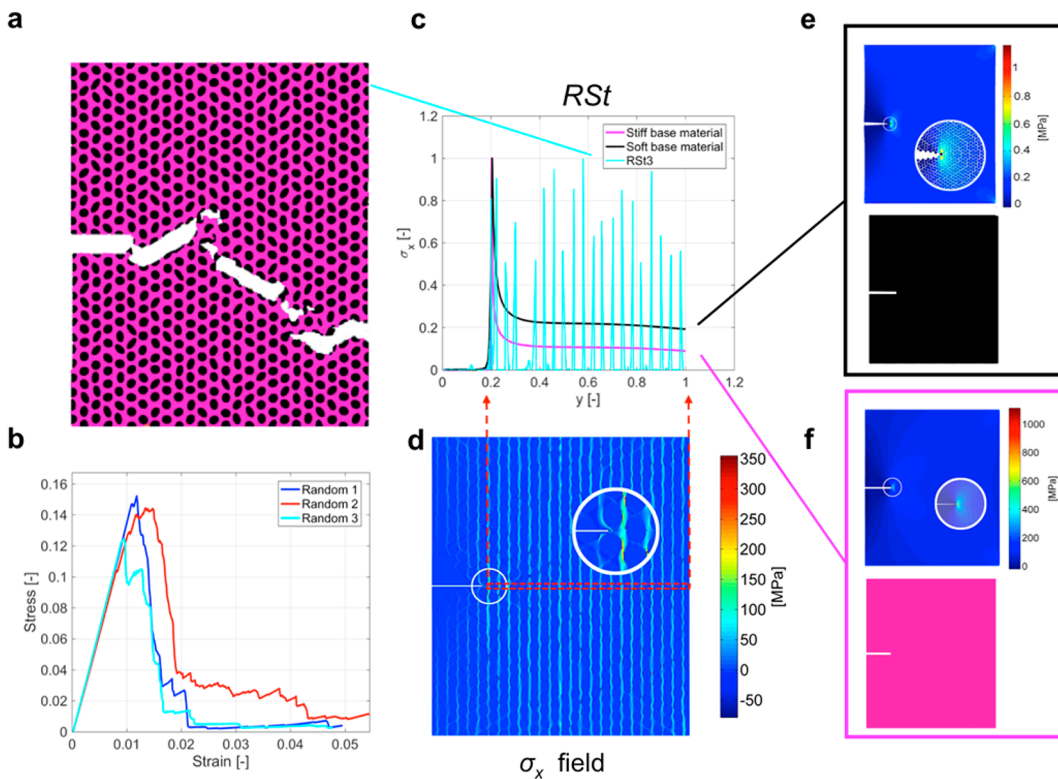


Figure 6. Effect of random topology. Composites with random topology and stiff matrix (*RSt*) demonstrate a higher defect tolerance. In this particular case, the highest stresses are located not at the crack tip, but in other areas, making this topology less sensitive to the presence of the crack. (a) Failure mode of one of the three composites with random topologies and stiff matrix, showing all the mechanisms observed in bone (i.e., crack deflection, matrix microcracking, fibril bridging, and uncracked-ligament bridging). (b) Stress–strain curves of the three *RSt* composites modeled; stresses are normalized with respect to the numerical strength of the stiff base material. (c) Stress (σ_x) trend from the crack tip to the far field showing delocalization of the maximum stresses and a large improvement in the defect tolerance with respect to the base materials and to the *CSt* topology. (d) Map of the stress (σ_x) field and zoom-in around the crack tip. Highlighted with red dashed lines the area where the stress, plotted in c, is calculated. The color bar indicates the magnitude of the stress in MPa. (e, f) Maps of the stress field in the (e) soft and (f) stiff base materials and schematic of the single-edge cracked homogeneous samples.

corresponding experimental and numerical strength of the stiff base material, we can observe a similar trend for experimental and numerical case studies. The aim of this normalization is to allow a direct comparison between numerical and experimental results. In both cases, the strength of the composites characterized by stiff matrix is about one-third of the stiff base material, whereas the strain is increased by 1 order of magnitude. This allows the composites to have more deformation and energy dissipation, thus yielding to a higher toughness modulus with respect to homogeneous materials.

Although the composites are made of the same building blocks and the same reinforcement ratio (60%), we can observe a wide range of stress–strain behaviors, as observed in previous experiments.¹⁵

3.2. Failure Modes. Figure 3 shows a comparison between the characteristic toughening mechanisms occurring in bone microstructure, and those observed in the bonelike composites. The numerical models accurately reproduce the typical bonelike toughening mechanisms (i.e., crack deflection, uncracked-ligament bridging, constrained microcracking, and fibril bridging), previously mimicked by the 3D-printed bioinspired patterns, and reproduce the failure modes of the experimental counterparts. An example is shown in Figure 4, for the *CSo* topology (circular reinforcement–soft matrix). Here, a comprehensive comparison between numerical and experimental results is given, in terms of stress–strain curve and failure mode for the *CSo*. For the other topologies a

comparison between numerical and experimental results is provided in Figures S3 and S4. The numerical model fails by crack deflection, as observed in the experiments. Moreover, there is a close similarity in the stress–strain trend, though a one order of magnitude difference is observed in stress because of the initially assigned properties (stiffness increased by one order of magnitude to reduce the computational effort).

As previously observed in the experiments, the composites characterized by soft matrix mainly failed by crack deflection (Figures 3d and 4a), whereas those characterized by stiff matrix mainly failed by uncracked-ligament bridging and fibril bridging (Figure 3a, b). The composites characterized by random topology and stiff matrix, named *RSt* (Figure 6a), show instead the mutual presence of all failure modes, making them more similar to the bone tissue. In these composites, the osteon volume fraction is 60%, as in the other bone-inspired composites and similar to the average one of bovine bone.²⁶ The randomness regards the dimensions, the shape (circular-to-elliptical), and the orientation of the osteons. We designed and tested three different types of *RSt* composites, which showed a similar failure mode and comparable mechanical performance (Figure 6b).

3.3. Defect Tolerance. The composites, characterized by soft reinforcement and stiff matrix (e.g., *CSt* and *ESt*), show higher strength and toughness (Figure 2) and a higher damage tolerance (Figure 5) compared to the designs made of soft matrix. As example, Figure 5 shows how the combination of

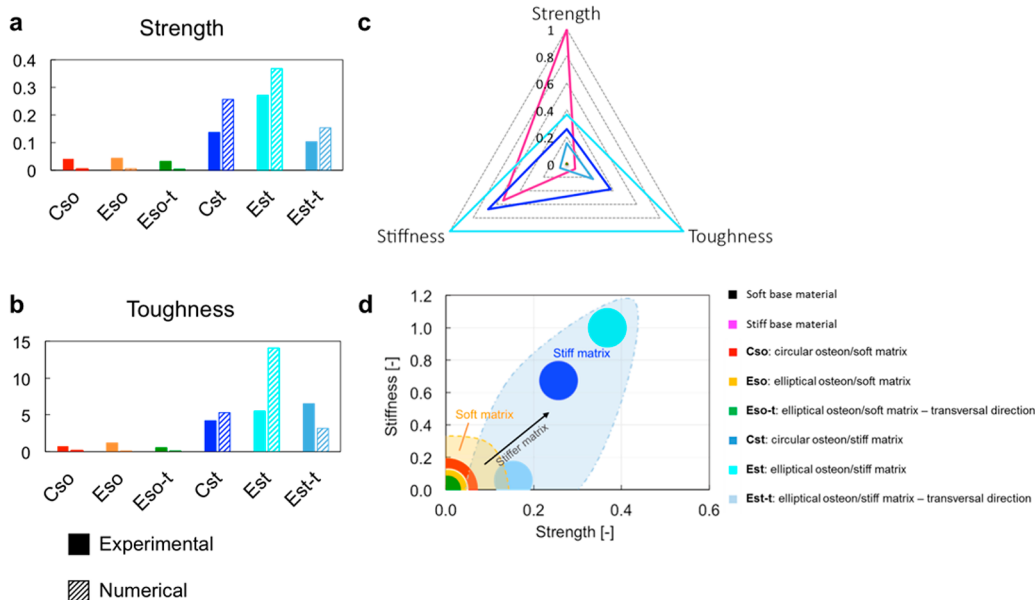


Figure 7. Prediction of the strength-toughness trend and of the optimal topology. Bar plot showing the comparison between numerical and experimental results in terms of (a) strength and (b) toughness values for various topologies. Data are normalized by the corresponding numerical and experimental values of the stiff base material for strength and toughness, respectively. (c) Radar plot showing a comparison among all topologies of samples. Data are normalized by the maximum value of each mechanical property. The “ESt” composite type (i.e., soft elliptical reinforcement/stiff matrix), tested under longitudinal loading, shows the best combination of mechanical properties (i.e., strength, toughness, stiffness), measured as the proportional area of the radar plots. (d) Ashby plot (Stiffness vs Strength) showing the positive effect of a stiffer matrix: here both the stiffness and the strength are normalized by the maximum value (among composites and base materials).

circular topology and stiff matrix (C_{St}) is beneficial for reducing the stress concentration at crack tip, especially if compared to the C_{SO} topology (circular osteon/soft matrix) and to the stiff and soft base materials. The pattern itself allows the stress delocalization (Figure 5a, c): indeed, although the maximum stress is located at the crack tip, other peak stresses can be identified at the reinforcement-matrix interface. In the case of C_{St}, besides the stress delocalization due to the circular pattern, we can also notice a reduced stress concentration at the crack tip with respect to the far field (Figure 5b), if compared to C_{SO} (Figure 5d) and to the homogeneous soft (Figure 5e) and stiff (Figure 5f) base materials, making the whole composite more damage tolerant.

The random topology has shown to be even more beneficial for defect tolerance. In particular, R_{St} (random pattern with stiff matrix) represents the best-case scenario for flaw tolerance (see Figure 6), compared to the other heterogeneous and homogeneous materials. Indeed, this case study is the closest to bone tissue, where we have an apparently random distribution of osteon with a circular-to-elliptical cross section, interspersed into a stiffer interstitial matrix.^{26,41} Figure 6b depicts the stress-strain behavior for the three R_{St} case-studies, which have a clear similarity. For the sake of brevity, in Figure 6 we only report the failure mode (Figure 6a), the stress σ_x trend from the crack tip (Figure 6c), and the stress σ_x distribution (Figure 6d) of one case, because of the similarity to the other two. In the R_{St} case studies, the combination of a random geometrical topology and random pattern with a stiff matrix allows for a stress delocalization and an enhanced damage tolerance. In particular, the peak stresses are located in the far field, making the composite less sensitive to the presence of a flaw. Indeed, the failure of this composite is not due to the propagation of the main crack, but to the combination of different progressive failure mechanisms (i.e., crack deflection, matrix microcracking,

fibril bridging, and uncracked-ligament bridging), as characteristic of bone tissue.

3.4. Prediction of the Strength-Toughness Trend and the Optimal Topology.

The bar plots, depicted in Figure 7a, b, show a similar trend of numerical and experimental results, in terms of strength (Figure 7a) and toughness (Figure 7b) values, for various topologies. Data are normalized by the respective numerical and experimental values of the stiff base material for strength and toughness, respectively, allowing a direct comparison between experimental and numerical results.

We observed an increase in toughness of the composites compared to the base materials, almost one order of magnitude, as represented by the radar plot in Figure 7c, where the data are normalized by the maximum value of each mechanical characteristic. According to this plot the “ESt” composite type (i.e., soft elliptical reinforcement/stiff matrix), tested under loading oriented along the main axis of the ellipses, has the best performance in terms of strength, toughness, and stiffness, measured as the proportional area of the radar plots, confirming the previous experimental findings.¹⁵ Furthermore, we noticed a positive effect of the stiff matrix in enhancing both strength and stiffness, as shown by the Ashby plot in Figure 7d.

4. DISCUSSION

The simulations presented allow one to get an insight into the mechanisms governing the failure process, and determining the final toughness of the composites. The visualization software, VMD,⁴² allows one to get snapshots revealing the primary deformation and toughening mechanisms, and videos, to follow the deformation and failure process. The material failure at the continuous level observed in our previous experiments is captured from the spring failure at the microdiscontinuous scale level of our model. The origin of such nonbrittle behavior may be related to our assumption of a triangular lattice with an equal

stiffness of springs having different orientations (e.g., parallel to the displacement direction and 60°-oriented). In this case, when we apply a displacement, initially the springs parallel to the load reach 100% deformation and break, then progressively those at 60° orientation. This simplification allowed us to provide a better approximation of the nonbrittle nature of our polymeric materials, and especially to the composite behavior, where we also have structure-related nonlinearity. A similar behavior has also been observed in previous papers, describing the response of inhomogeneous materials and bioinspired structures through mesoscale models with triangular lattice.^{20,30,38,47} The postprocessing of results, and in particular the stress-maps and the stress trend from the crack tip to the far field, provide further understandings into the role of the topological pattern and the stiffness ratio (stiffness of reinforcement vs stiffness of the matrix). In particular, we notice how the toughening mechanisms and the resulting performance depend on both the heterogeneity of the material (reinforcement and matrix properties) and the composite topology. The heterogeneity (i.e., composite nature) and the disorder (i.e., random topology) have shown to be beneficial, promoting stress delocalization, whereas a stiffer matrix, which corresponds to a lower stiffness ratio (reinforcement s. vs matrix st.), has a crucial role in fostering damage tolerance. It is interesting to note that the heterogeneity, the disorder, though apparent, and the stiffer matrix are all distinguishing features of bone tissue.^{26,41,43,44}

The advantage of the proposed framework is to provide a comprehensive analysis of the material, allowing one to make estimations on the material performance, necessary for a requirement-base design, but also to get a deep understanding of the material behavior from a mechanistic point of view. Not only can one predict the material with the best performance but the user will also be able to unravel the reasons behind that. This represents an added value for a design tool, embracing the different needs of the design process.

5. CONCLUSION

With the advent of additive manufacturing, there is an increasing demand of computational tools able to guide the design phase. Here, we propose a numerical framework, built on a 2D lattice spring model where the material is discretized into spring-connected beads, and validated based on previous experimental outcomes.¹⁵ Thus, it represents a fundamental and reliable tool for material design. The developed computational framework is able to accurately reproduce the toughening mechanisms and the failure modes experimentally observed, and it constitutes a useful tool to estimate the mechanical performance of various composites. Although it cannot provide an exact estimation of the properties, because of initial hypotheses intrinsic to the model, it is able to reproduce the trend of mechanical properties, making it an invaluable instrument for engineering design. Moreover, it allows one to have an insight into the deformation and toughening mechanisms, unraveling the role of the topologies and the materials (i.e., stiffness ratio) in enhancing the toughness and promoting damage tolerance.

In future work, we aim to reduce the computational cost, performing simulations on single unit cells. The simulations performed on single unit cells can be useful for an estimation of the properties (in the case of a regular pattern), whereas the full-scale models allow one to perform an *in silico* test, which is a replica of the experimental one. With the support of a valid

numerical framework, we can think of tuning the mechanics of a material by simply changing its geometry and arrangement. The random topology proposed in this paper is an example of augmented flaw tolerance, which may be further improved in future studies, perhaps including gradient features to adapt the material response to varying loading conditions. Having the ability of tailoring the mechanics of a material by fine-tuning its geometry represents the future challenge of additive manufacturing, which may provide proof-of-concept design solutions for diverse applications. Going forward, the material design could be adjusted to meet specific requirements leveraging optimization techniques.

■ ASSOCIATED CONTENT

S Supporting Information

The Supporting Information is available free of charge on the ACS Publications website at DOI: [10.1021/acsbiomaterials.7b00606](https://doi.org/10.1021/acsbiomaterials.7b00606).

Model framework, Figures S1–S4, and Tables S1–S4 ([PDF](#))

■ AUTHOR INFORMATION

Corresponding Author

*E-mail: mbuehler@mit.edu.

ORCID

Markus J. Buehler: [0000-0002-4173-9659](https://orcid.org/0000-0002-4173-9659)

Author Contributions

F.L., L.V., and M.J.B. designed the research. F.L. and V.C. performed the simulations. F.L., V.C., L.V., and M.J.B. analyzed and discussed the results. F.L., L.V., and M.J.B. wrote the paper with input from all coauthors. All authors reviewed the manuscript.

Notes

The authors declare no competing financial interest.

■ ACKNOWLEDGMENTS

The authors acknowledge support from “Progetto Rocca—MISTI Global seed funds”. F.L. acknowledges support from Young Researcher Fellowship. High performance computing resources have been provided by CINECA, through the ISCRA initiative. Additional support is acknowledged from ONR (N000141612333). The authors would like to thank Dr. Zhao Qin for insightful discussions and Marco Bellù for his help with the initial simulations.

■ REFERENCES

- (1) Wegst, U. G. K.; Bai, H.; Saiz, E.; Tomsia, A. P.; Ritchie, R. O. Bioinspired structural materials. *Nat. Mater.* **2015**, *14* (1), 23–36.
- (2) Wegst, U. G. K.; Ashby, M. F. The mechanical efficiency of natural materials. *Philos. Mag.* **2004**, *84* (21), 2167–2186.
- (3) Libonati, F.; Buehler, M. J. Advanced Structural Materials by Bioinspiration. *Adv. Eng. Mater.* **2017**, *19* (5), 1600787.
- (4) Espinosa, H. D.; Rim, J. E.; Barthelat, F.; Buehler, M. J. Merger of structure and material in nacre and bone - Perspectives on de novo biomimetic materials. *Prog. Mater. Sci.* **2009**, *54* (8), 1059–1100.
- (5) Barthelat, F.; Yin, Z.; Buehler, M. J. Structure and mechanics of interfaces in biological materials. *Nature Reviews Materials* **2016**, *1*, 16007.
- (6) Barthelat, F.; Rabiei, R. Toughness amplification in natural composites. *J. Mech. Phys. Solids* **2011**, *59* (4), 829–840.
- (7) Sun, J.; Bhushan, B. Hierarchical structure and mechanical properties of nacre: a review. *RSC Adv.* **2012**, *2* (20), 7617–7632.

- (8) Currey, J. D. Materials science: hierarchies in biomimetic structures. *Science* **2005**, *309*, 253.
- (9) Lakes, R. Materials with structural hierarchy. *Nature* **1993**, *361* (6412), 511–515.
- (10) Rho, J. Y.; Kuhn-Spearing, L.; Ziopoulos, P. Mechanical properties and the hierarchical structure of bone. *Med. Eng. Phys.* **1998**, *20*, 92.
- (11) Libonati, F. Bio-inspired Composites: Using Nature to Tackle Composite Limitations. In *Advanced Engineering Materials and Modeling*; John Wiley & Sons: New York, 2016; pp 165–190.
- (12) Fratzl, P. Biomimetic materials research: What can we really learn from nature's structural materials? *J. R. Soc., Interface* **2007**, *4*, 637.
- (13) Ritchie, R. O. The conflicts between strength and toughness. *Nat. Mater.* **2011**, *10* (11), 817–22.
- (14) Lapidot, S.; Meirovitch, S.; Sharon, S.; Heyman, A.; Kaplan, D. L.; Shoseyov, O. Clues for biomimetics from natural composite materials. *Nanomedicine (London, U.K.)* **2012**, *7* (9), 1409–23.
- (15) Libonati, F.; Gu, G. X.; Qin, Z.; Vergani, L.; Buehler, M. J. Bone-Inspired Materials by Design: Toughness Amplification Observed Using 3D Printing and Testing. *Adv. Eng. Mater.* **2016**, *18* (8), 1354–1363.
- (16) Libonati, F.; Colombo, C.; Vergani, L. Design and characterization of a biomimetic composite inspired to human bone. *Fatigue Fract. Eng. Mater. Struct.* **2014**, *37* (7), 772–781.
- (17) Libonati, F.; Vergani, L. Cortical Bone as a Biomimetic Model for the Design of New Composites. *Procedia Structural Integrity* **2016**, *2*, 1319–1326.
- (18) Dimas, L. S.; Bratzel, G. H.; Eylon, I.; Buehler, M. J. Tough Composites Inspired by Mineralized Natural Materials: Computation, 3D printing, and Testing. *Adv. Funct. Mater.* **2013**, *23*, 4629–4638.
- (19) Martin, J. J.; Fiore, B. E.; Erb, R. M. Designing bioinspired composite reinforcement architectures via 3D magnetic printing. *Nat. Commun.* **2015**, *6*, 8641.
- (20) Mirzaifar, R.; Dimas, L. S.; Qin, Z.; Buehler, M. J. Defect-Tolerant Bioinspired Hierarchical Composites: Simulation and Experiment. *ACS Biomater. Sci. Eng.* **2015**, *1* (5), 295–304.
- (21) Mirzaali, M. J.; Mussi, V.; Vena, P.; Libonati, F.; Vergani, L.; Strano, M. Mimicking the loading adaptation of bone microstructure with aluminum foams. *Mater. Des.* **2017**, *126*, 207–218.
- (22) Rajasekharan, A. K.; Bordes, R.; Sandström, C.; Ekh, M.; Andersson, M. Hierarchical and Heterogeneous Bioinspired Composites—Merging Molecular Self-Assembly with Additive Manufacturing. *Small* **2017**, *13*, 1700550.
- (23) Gu, G. X.; Libonati, F.; Wettermark, S.; Buehler, M. J. Printing Nature: Unraveling the Role of Nacre's Mineral Bridges. *J. Mech. Behav. Biomed. Mater.* **2017**, in press; DOI: [10.1016/j.jmbbm.2017.05.007](https://doi.org/10.1016/j.jmbbm.2017.05.007).
- (24) Gu, G. X.; Dimas, L.; Qin, Z.; Buehler, M. J. Optimization of Composite Fracture Properties: Method, Validation, and Applications. *J. Appl. Mech.* **2016**, *83* (7), 071006–071006.
- (25) Kokkinis, D.; Schaffner, M.; Studart, A. R. Multimaterial magnetically assisted 3D printing of composite materials. *Nat. Commun.* **2015**, *6*, 8643.
- (26) Abdel-Wahab, A. A.; Maligno, A. R.; Silberschmidt, V. V. Microscale modelling of bovine cortical bone fracture: Analysis of crack propagation and microstructure using X-FEM. *Comput. Mater. Sci.* **2012**, *52* (1), 128–135.
- (27) Djumas, L.; Molotnikov, A.; Simon, G. P.; Estrin, Y. Enhanced Mechanical Performance of Bio-Inspired Hybrid Structures Utilising Topological Interlocking Geometry. *Sci. Rep.* **2016**, *6*, 26706.
- (28) Curtin, W. A.; Scher, H. Brittle fracture in disordered materials: A spring network model. *J. Mater. Res.* **1990**, *5* (3), 535–553.
- (29) Buxton, G. A.; Care, C. M.; Cleaver, D. J. A lattice spring model of heterogeneous materials with plasticity. *Modell. Simul. Mater. Sci. Eng.* **2001**, *9* (6), 485.
- (30) Sen, D.; Buehler, M. J. Structural hierarchies define toughness and defect-tolerance despite simple and mechanically inferior brittle building blocks. *Sci. Rep.* **2011**, *1*, [10.1038/srep00035](https://doi.org/10.1038/srep00035).
- (31) Budyn, É.; Hoc, T. Multiple scale modeling for cortical bone fracture in tension using X-FEM. *European Journal of Computational Mechanics/Revue Européenne de Mécanique Numérique* **2007**, *16* (2), 213–236.
- (32) Gu, G. X.; Su, I.; Sharma, S.; Voros, J. L.; Qin, Z.; Buehler, M. J. Three-Dimensional-Printing of Bio-Inspired Composites. *J. Biomech. Eng.* **2016**, *138* (2), 021006–021006.
- (33) Tran, P.; Ngo, T. D.; Ghazlan, A.; Hui, D. Bimaterial 3D printing and numerical analysis of bio-inspired composite structures under in-plane and transverse loadings. *Composites, Part B* **2017**, *108*, 210–223.
- (34) Vergani, L.; Colombo, C.; Libonati, F. Crack Propagation in Cortical Bone: A Numerical Study. *Procedia Mater. Sci.* **2014**, *3* (0), 1524–1529.
- (35) Feerick, E. M.; Liu, X.; McGarry, P. Anisotropic mode-dependent damage of cortical bone using the extended finite element method (XFEM). *Journal of the Mechanical Behavior of Biomedical Materials* **2013**, *20*, 77–89.
- (36) Tanaka, Y. Reduced stress concentration and enhanced fracture toughness by yielding-rehardening combination. *Eur. Phys. J. E: Soft Matter Biol. Phys.* **2012**, *35* (3), 23.
- (37) Brely, L.; Bosia, F.; Pugno, N. M. A Hierarchical Lattice Spring Model to Simulate the Mechanics of 2-D Materials-Based Composites. *Front. Mater.* **2015**, *2*, 51.
- (38) Dimas, L. S.; Buehler, M. J. Modeling and additive manufacturing of bio-inspired composites with tunable fracture mechanical properties. *Soft Matter* **2014**, *10* (25), 4436–4442.
- (39) Dimas, L. S.; Buehler, M. J. Influence of geometry on mechanical properties of bio-inspired silica-based hierarchical materials. *Bioinspiration Biomimetics* **2012**, *7* (3), 036024.
- (40) Ritchie, R. O.; Buehler, M. J.; Hansma, P. Plasticity and toughness in bone. *Phys. Today* **2009**, *62* (6), 41–47.
- (41) Abdel-Wahab, A.; Silberschmidt, V. V. Plastic behaviour of microstructural constituents of cortical bone tissue: a nanoindentation study. *Int. J. Exp. Computat. Biomech.* **2013**, *2* (2), 136.
- (42) Humphrey, W.; Dalke, A.; Schulter, K. VMD: Visual molecular dynamics. *J. Mol. Graphics* **1996**, *14* (1), 33–38.
- (43) Tai, K.; Dao, M.; Suresh, S.; Palazoglu, A.; Ortiz, C. Nanoscale heterogeneity promotes energy dissipation in bone. *Nat. Mater.* **2007**, *6* (6), 454–462.
- (44) Phelps, J. B.; Hubbard, G. B.; Wang, X.; Agrawal, C. M. Microstructural heterogeneity and the fracture toughness of bone. *J. Biomed. Mater. Res.* **2000**, *51*, 735–41.
- (45) Tsai, D. H. The virial theorem and stress calculation in molecular dynamics. *J. Chem. Phys.* **1979**, *70* (3), 1375–1382.
- (46) Zimmerman, J. A.; WebbIII, E. B.; Hoyt, J. J.; Jones, R. E.; Klein, P. A.; Bammann, D. J. Calculation of stress in atomistic simulation. *Modell. Simul. Mater. Sci. Eng.* **2004**, *12* (4), S319.
- (47) Beale, P. D.; Srolovitz, D. J. Elastic fracture in random materials. *Phys. Rev. B: Condens. Matter Mater. Phys.* **1988**, *37* (10), 5500–5507.